Antitumor effects and mechanisms of pyropheophorbide-α methyl ester-mediated photodynamic therapy on the human osteosarcoma cell line MG-63

YANYANG CHEN*, HANG YIN*, YONG TAO, SHENXI ZHONG, HAOYANG YU, JIANXIAO LI, ZHIBIAO BAI and YUNSHENG OU

Department of Orthopedics, The First Affiliated Hospital of Chongqing Medical University, Chongqing 400016, P.R. China

Received August 10, 2018; Accepted November 20, 2019

DOI: 10.3892/ijmm.2020.4494

Abstract. Photodynamic therapy (PDT) is a promising treatment for osteosarcoma, and pyropheophorbide-α methyl ester (MPPa) is a second-generation photosensitizer for tumor treatment. The present study aimed to determine the efficacy and possible mechanisms of MPPa-PDT in the treatment of osteosarcoma MG-63 cells. Flow cytometry and western blotting were used to detect cell cycle-related indicators Cyclin D1, Cyclin E, Cyclin A and Cyclin B1. Cell migration and invasion abilities were detected using wound-healing and Transwell chamber assays. Cellular endoplasmic reticulum stress (ERS), autophagy and apoptosis-related indicators were detected by flow cytometry and western blotting. The results demonstrated that MPPa-PDT blocked the MG-63 cell cycle and inhibited cell migration and invasion. Additionally, MPPa-PDT inhibited the activation of the Akt/mammalian target of rapamycin (mTOR) pathway. MG-63 cells underwent ERS-induced apoptosis following MPPa-PDT treatment. Pretreatment with the mTOR phosphorylation inhibitor rapamycin affected the autophagy of MPPa-PDT-induced osteosarcoma MG-63 cells and enhanced apoptosis through targeting mTOR.

Introduction

Osteosarcoma is the most common primary malignant bone tumor in clinical practice; these tumors exhibit strong local invasiveness, can easily metastasize at an early stage, and have a poor prognosis (1-3). Osteosarcoma occurs mainly in children and adolescents, and the 5-year survival rate is 65-75% (1). Recent advances in surgery, radiotherapy and neoadjuvant chemotherapy have greatly improved the prognosis of osteosarcoma, but recurrence, metastasis, and drug resistance still result in a poor prognosis. In addition, surgical resection severely impairs the limb function of the patients, and radiotherapy and chemotherapy are limited due to their severe systemic toxicity (2). Therefore, the development of new anti-osteosarcoma treatments with fewer complications and side effects is urgently required (3).

Photodynamic therapy (PDT) is a new method for tumor treatment that has the advantages of high selectivity, limited damage, low toxicity, few side effects and reproducibility (4,5). In addition, its curative effect is improved when combined with surgery (6). PDT has been used for various malignant diseases, including breast, gastric and skin cancer (7-10). In PDT, a photosensitizer is infused intravenously or injected locally into the body to ensure that the photosensitizer is relatively enriched specifically in the tumor tissue; then, the tumor tissue is locally irradiated with light of a corresponding wavelength. When the photosensitizer is excited by the light, photochemical and photobiological reactions in the surrounding environment produce large amounts of reactive oxygen species (ROS), which destroy tumor cells and tissues, leading to tumor cell death (11-13). Early PDT methods used mainly hematoporphyrin derivatives as photosensitizers. These photosensitizers are slowly metabolized by the body, which leads to long periods during which light must be avoided after treatment; additionally, their composition is complex, the targeting is weak and their skin phototoxicity is strong (14-16). Pyropheophorbide-α methyl ester (MPPa) belongs to the second generation of photosensitizers; this novel type of photosensitizer exhibits strong photosensitivity, a clear chemical structure, a single component and a stable nature, and it is metabolized rapidly by the body (17-19). MPPa-PDT has been studied in multiple types of cancer such as breast, lung and prostate cancer (20-22). de Miguel *et al* (23) have reported that photodynamic therapy is a potential antitumoral treatment for surgically inoperable osteosarcoma. However, further study of its mechanism for treating osteosarcoma is required.

Correspondence to: Professor Yunsheng Ou, Department of Orthopedics, The First Affiliated Hospital of Chongqing Medical University, 1 Youyi Road, Yuzhong, Chongqing 400016, P.R. China
E-mail: ouyunsheng2001@163.com

*Contributed equally

Key words: pyropheophorbide-α methyl ester, photodynamic therapy, osteosarcoma, cell cycle, migration, invasion, p-mTOR, apoptosis

The present study aimed to explore the effects of MPPa-PDT on the cell cycle, migration and invasion of human osteosarcoma MG-63 cells. MPPa-PDT-induced apoptosis in osteosarcoma MG-63 cells and the related mechanisms were examined to provide an experimental basis for the clinical treatment of osteosarcoma.

Materials and methods

Cell lines and reagents. The MG-63 cell line was purchased from. The human fibroblast HFL-1 cell line was donated by Professor Zhou Jing, Department of Respiratory, the First Affiliated Hospital of Chongqing Medical University (Chongqing, China). MPPa and rapamycin (RAPA) were purchased from Sigma-Aldrich; Merck KGaA. Dulbecco's modified Eagle's medium (DMEM) and Matrigel were obtained from BD Biosciences. Fetal bovine serum (FBS) and trypsin were purchased from Gibco; Thermo Fisher Scientific, Inc. FLUO-3/AM was purchased from Dojindo Molecular Technologies, Inc. An Annexin V-propidium iodide (PI) double-staining test kit was purchased from Nanjing Keygen Biotech Co., Ltd. Cyclin D1, Cyclin E, Cyclin A, Cyclin B1, E-cadherin (E-cad), MMP-2, MMP-9, Akt, phosphorylated (p)-Akt, mTOR, p-mTOR, 4EBP1, eukaryotic translation initiation factor 4E-binding protein 1 (4EBP1), p-4EBP1, P70S6K, p-P70S6K, Bip, serine/threonine-protein kinase/endoribonuclease IRE1 (IRE1α), eukaryotic translation initiation factor 2α kinase 3 (PERK), protein disulfide isomerase (PDI), C/EBP-homologous protein 10 (CHOP), cleaved caspase-3, cleaved poly (ADP-ribose) polymerase 1 (PARP), microtubule-associated protein 1 light chain 3α (LC-3), P62 and β-actin antibodies were purchased from Cell Signaling Technology, Inc. A cleaved caspase-12 antibody was purchased from Wuhan Sanying Biotechnology, and a p-PERK antibody was supplied by Santa Cruz Biotechnology. The PDT equipment was purchased from Chongqing Jingyu Laser Technology Co. Ltd.

Experimental grouping and processing. The experiment comprised six groups as follows: i) Control, untreated cells; ii) MPPa, cells treated with MPPa alone; iii) LED, cells treated with a light-emitting diode (LED) alone; iv) RAPA, cell treated with RAPA alone; v) MPPa-PDT, cell treated with MPPa and light; and vi) MPPa-PDT-RAPA, cells treated with MPPa, RAPA and light. MG-63 cells were placed in complete medium containing 10% FBS, 90% DMEM and 100 μg/ml penicillin and streptomycin and cultured at 37˚C in a 5% CO_2 incubator. Upon reaching the logarithmic growth phase, the medium was changed. RAPA (20 ng/ml) was added in the dark to the RAPA and MPPa-PDT-RAPA groups, MPPa (0.75 μmol/l) was added in the dark to the MPPa, MPPa-PDT and MPPa-PDT-RAPA groups, and equal volumes of complete medium were added in the dark to the control and LED groups. Each group was incubated in a 37˚C and 5% CO_2 incubator for 20 h in the dark; subsequently, the cultures were washed twice with PBS, and complete medium was added. The LED, MPPa-PDT and MPPa-PDT+RAPA groups were irradiated for 120 sec with an integrated LED special light source (wavelength, 630 nm; continuous output mode; optical power density, 40 mW/cm^2) to provide the cells with a light dose of 4.8 J/cm^2 based on a previous study, which demonstrated that at a light dose of 4.8 J/cm^2, the inhibition rate of the group that received 0.75 μmol/l MPPa was 48.6±2.71% (9). Following treatment, cells were collected for subsequent experiments.

Cytotoxicity assay. The anti-proliferative effects of MPPa on human fibroblast HFL-1 cells was assessed by Cell Counting Kit-8 (CCK-8) assay (MedChemExpress LLC). Cells were treated with various concentrations of MPPa (0, 0.5, 0.75 and 1.0 μmol/l) for 24 h. Subsequently, 10 μl CCK-8 was added to each well, and the plates were incubated for 1-2 h at 37˚C according to the manufacturer's instructions. A microplate reader was used to detect the absorbance at 450 nm. Data represented the mean of five replicates. Cell viability was calculated using the following equation: Cell viability (%)=Average OD in study group/average OD in control group x100%, where OD was the optical density. Each assay was performed in triplicate. Based on the results of the cell viability assay (Fig. S1), an appropriate MPPa concentration was selected for subsequent experiments.

Cell cycle assay. Human osteosarcoma MG-63 cells in the logarithmic growth phase were inoculated into 6-well plates at a density of 2x10^6 cells/well, and the control and experimental groups were established. Each group was placed in 3 replicate wells that were treated with MPPa, LED or MPPa-PDT for 12 h, and the supernatants were discarded. Following clearing and washing once with PBS, the cells were collected, resuspended in 70% ice-cold ethanol, fixed at 4˚C overnight and centrifuged at 1,000 x g for 5 min at 4˚C. Cells were washed once with 1 ml PBS, and 500 μl PBS containing 50 μg/ml PI, 100 μg/ml RNase A and 0.2% Triton X-100 was added and incubated for 30 min at 4˚C in the dark. The fixation solution was discarded, and the cells were resuspended in an appropriate amount of PBS and subjected to cell cycle detection using CytoFLEX flow cytometer with CytExpert 2.1 software (Beckman Coulter, Inc.).

Wound-healing assay. Osteosarcoma MG-63 cells in the logarithmic growth phase were seeded into 6-well plates (2x10^6 cells/well). After 70% confluence was reached in each group, MPPa (0.75 μmol/l) was added to the MPPa and MPPa-PDT groups. Following 20-h MPPa treatment, a 10-μl pipette tip was used to make a scratch in the cell monolayer. The wells were washed three times with PBS to remove the floating cells, and 2 ml serum-free culture medium was added to each group. The LED and MPPa-PDT groups were treated with LED irradiation. Then, the plates were placed in a 37˚C and 5% CO_2 incubator. After 24 h, cell migration was observed under an inverted light microscope, and the wells were photographed to measure the scratch width using Image J 2.1.4 (National Institutes of Health).

Transwell invasion assay. Transwell chambers were placed in 24-well plates. Matrigel diluted in serum-free medium (1:8) was added to the upper chambers (100 μl per chamber), and the plates were placed in 37˚C with 5% CO_2 for 2 h. A total of 100 μl (3x10^5 cells/ml) MG-63 cell suspension with or without MPPa (0.75 μmol/l) was added to the

Table I. Antibody details.

Protein name	Source	Cat. no.	Dilution	Secondary antibody
Cyclin D1	CST	2978	1:1,000	Anti-rabbit
Cyclin E	CST	20808	1:1,000	Anti-rabbit
Cyclin A	CST	4656	1:2,000	Anti-mouse
Cyclin B1	CST	12231	1:1,000	Anti-rabbit
E-cadherin	CST	3195	1:1,000	Anti-rabbit
MMP-2	CST	40994	1:1,000	Anti-rabbit
MMP-9	CST	13667	1:1,000	Anti-rabbit
Akt	CST	4691	1:1,000	Anti-rabbit
p-Akt	CST	4060	1:2,000	Anti-rabbit
mTOR	CST	2983	1:1,000	Anti-rabbit
p-mTOR	CST	5536	1:1,000	Anti-rabbit
4EBP1	CST	9644	1:1,000	Anti-rabbit
p-4EBP1	CST	2855	1:1,000	Anti-rabbit
P70S6K	CST	2708	1:1,000	Anti-rabbit
p-P70S6K	CST	9208	1:1,000	Anti-rabbit
Bip	CST	3177	1:1,000	Anti-rabbit
IRE1α	CST	3294	1:1,000	Anti-rabbit
PERK	CST	5683	1:1,000	Anti-rabbit
Protein disulfide	CST	3501	1:1,000	Anti-rabbit
CHOP	CST	2895	1:1,000	Anti-mouse
Cleaved caspase-3	CST	9664	1:1,000	Anti-rabbit
Cleaved PARP	CST	5625	1:1,000	Anti-rabbit
LC-3	CST	13118	1:1,000	Anti-rabbit
P62	CST	23214	1:1,000	Anti-rabbit
p-PERK	Santa Cruz	Sc-32577	1:1,000	Anti-rabbit
β-actin	CST	4970	1:1,000	Anti-rabbit
Goat-anti-rabbit	Invitrogen	G-21040	1:10,000	
Goat-anti-mouse	Invitrogen	31430	1:10,000	

MMP, matrix metallopeptidase; 4EBP1, eukaryotic translation initiation factor 4E-binding protein 1; IRE1α, serine/threonine-protein kinase/endoribonuclease IRE1; PERK, eukaryotic translation initiation factor 2α kinase 3; CHOP, C/EBP-homologous protein 10; PARP, poly (ADP-ribose) polymerase 1; LC-3, microtubule-associated protein 1 light chain 3α; p, phosphorylated; CST, Cell Signaling Technology, Inc.

upper chambers, and the LED and MPPa-PDT groups were serum-starved and treated with MPPa for 20 h. Following light irradiation, 1 ml medium containing 10% FBS was added to the lower chambers. After incubation for 48 h at 37˚C in a 5% CO_2 incubator, the chambers were removed, and the uninvaded cells in the upper chambers and the Matrigel were carefully wiped away with a cotton swab. The invading cells that had passed through the membrane were fixed with 100% methanol for 5 min at room temperature, stained with crystal violet for 15 min at room temperature and counted using an Olympus upright light microscope. The experiment was repeated three times.

Detection of intracellular calcium levels by flow cytometry. MG-63 cells in the logarithmic growth phase were inoculated at a density of 2x10^6 cells/well into 6-well culture plates, incubated for 20 h at 37˚C with 5% CO_2, treated according to their group and maintained for 2 h at 37˚C in the dark. Cells were collected and washed three times with PBS. The calcium ion fluorescent probe FLUO-3/AM (5 μmol/l in DMSO) was added to the cells and incubated at 37˚C for 15 min in the dark. Cells were washed three times with PBS and collected to make single-cell suspensions. The intracellular fluorescence intensity measured by flow cytometry (CytoFLEX flow cytometer; CytExpert 2.1) represented the calcium ion level.

Apoptosis measurement by flow cytometry. MG-63 cells were seeded into 6-well plates at a density of 2x10^6 cells/well. Suspended and adherent cells were collected after treatment and analyzed with an Annexin V/PI apoptosis kit. Briefly, 5 μl PI and FITC-labeled Annexin V was added to the cells, followed by mixing and incubation for 15 min at room temperature in the dark. Subsequently, 400 μl 1X binding buffer was added, and the cells were analyzed by flow cytometry (CytoFLEX flow cytometer; CytExpert 2.1).

Western blotting. After MG-63 cells in the logarithmic growth phase were treated according to their group, the

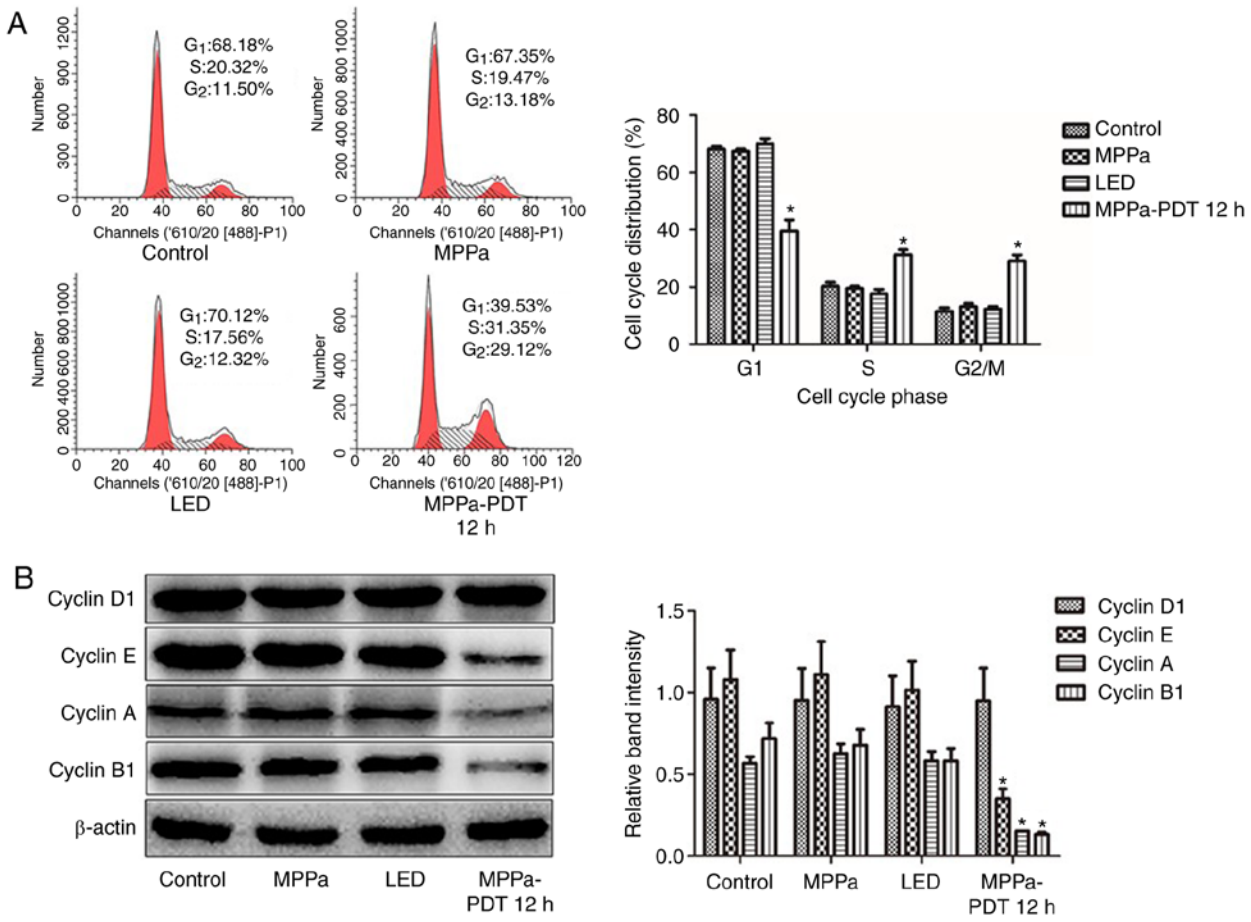

Figure 1. MPPa-PDT induces MG-63 cell cycle arrest. (A) After MPPa-PDT treatment for 12 h, the cell cycle was analyzed by flow cytometry. (B) At 12 h, whole-cell lysates were prepared to determine Cyclin D1, Cyclin E, Cyclin A and Cyclin B1 protein expression by western blotting. Data are presented as the means ± SD from three independent experiments. *P<0.05 vs. control. MPPa, pyropheophorbide-α methyl ester; PDT, photodynamic therapy; LED, cells treated with a light-emitting diode.

cells in were collected, and total protein was extracted using RIPA cell lysate (Sigma-Aldrich; Merck KGaA). The protein concentrations were determined using the bicinchoninic acid assay method (5 g/l), and 30 μg total protein per sample was used after boiling and denaturation. Following 10% SDS-PAGE, the PVDF membranes were incubated with 5% milk [non-fat milk powder in TBS +0.05% Tween-20 (TBST)] at room temperature for 10 min, and the corresponding primary antibodies were then added and incubated at 4˚C overnight. After rewarming in room temperature for 30 min, the membranes were rinsed four times with TBST (10 min/rinse), and a horseradish peroxidase-labeled secondary antibody was added to the blots and incubated for 1.5 h at room temperature. Following washing with TBST, the images were analyzed by ECL chemiluminescence using Quantity One 4.6.2 software. The antibody information in Table I.

Statistical analysis. The data are presented as the mean ± SD, and statistical comparisons were performed using one-way ANOVA with Dunnett's test. All statistical analyses were performed using SPSS software (version 22.0; IBM Corp.). Each experiment was repeated at least three times. The statistical significance tests were two-tailed. P<0.05 was considered to indicate a statistically significant difference.

Results

MPPa-PDT induces MG-63 cell cycle arrest. Previous studies reported that MPPa-PDT inhibited MG-63 cell proliferation (13). Therefore, the present study used flow cytometry to evaluate whether MPPa-PDT blocked cell proliferation by affecting the cell cycle. Compared with the proportions in the control, MPPa and LED groups, the proportion of cells in the G_1 phase significantly decreased, the proportion of cells in the G_2/M phase significantly increased and the proportion of cells in the S phase significantly increased in the MPPa-PDT group (P<0.05; Fig. 1A). No significant changes in the cell cycle ratios were observed among the control, MPPa and LED groups (P>0.05; Fig. 1A).

To investigate the mechanism of MPPa-PDT-induced cell cycle arrest, western blotting analysis was performed. Cyclin D1 and Cyclin E are essential proteins in the G_1 phase of cells, and Cyclin A and Cyclin B1 are key proteins in G_2/M phase. Cyclin E, Cyclin A and Cyclin B1 protein expression levels were significantly lower in the MPPa-PDT group compared with those in the control, MPPa and LED groups (P<0.05; Fig. 1B), whereas Cyclin D1 protein expression was not significantly different (P>0.05; Fig. 1B). No significant differences were observed in protein expression among the control, MPPa and

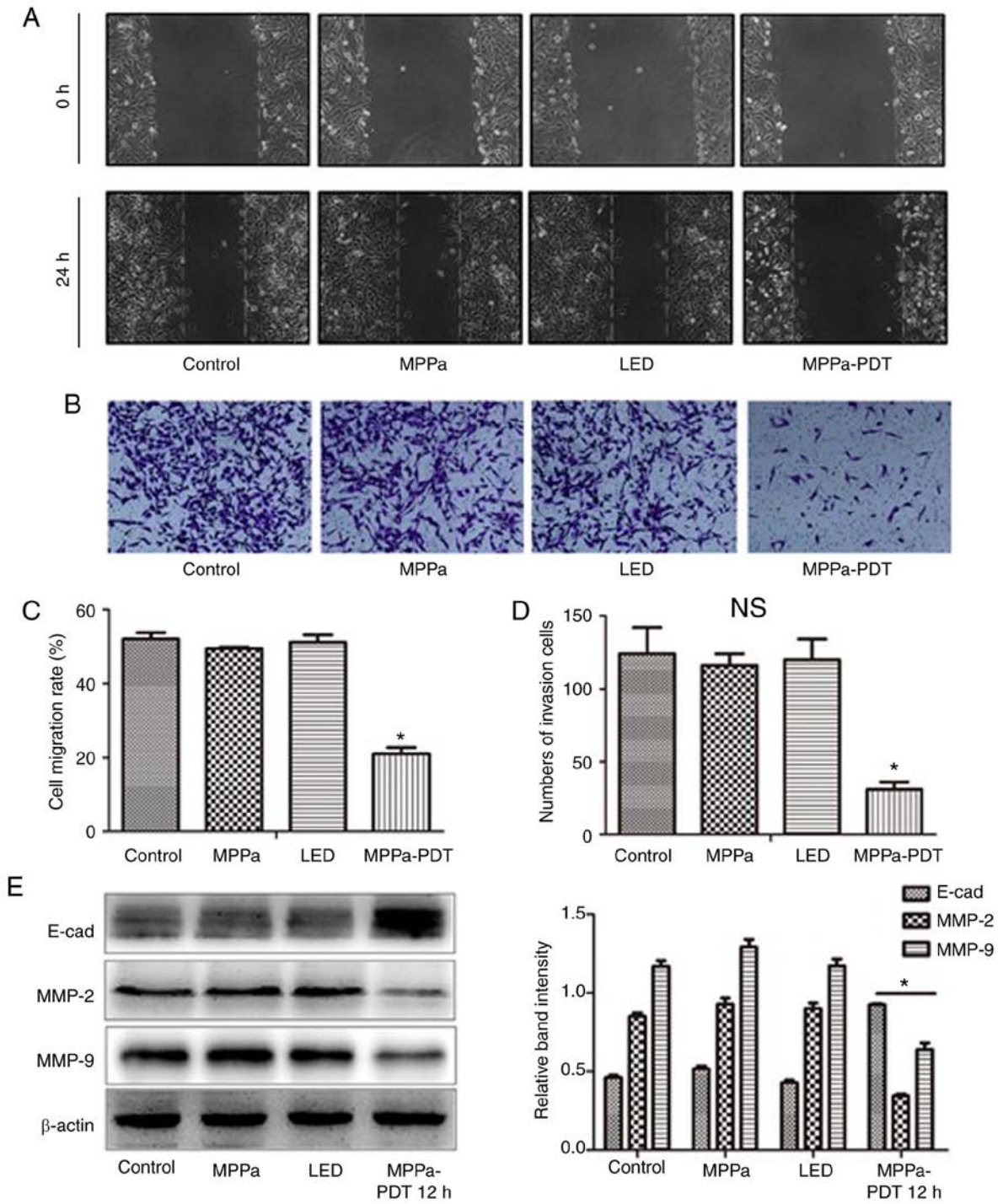

Figure 2. MPPa-PDT treatment inhibits MG-63 cell migration and invasion. (A) Cell migration was examined using wound-healing assays. (B) Cell invasion was detected using Matrigel-coated Transwell cell culture chambers. (C) The cell migration rates were counted in five random fields to evaluate the migratory ability of the MG-63 cells, and the data are expressed as the means ± SD. (D) The invasive ability of MG-63 cells was evaluated by counting the number of cells that invaded the lower surface of the membranes using a phase-contrast microscope (magnification, x100). (E) At 12 h, whole-cell lysates were prepared to determine E-cad, MMP-2 and MMP-9 protein expression by western blotting. The data are presented as the mean ± SD from three independent experiments. *P<0.05 vs. control. MPPa, pyropheophorbide-α methyl ester; PDT, photodynamic therapy; LED, cells treated with a light-emitting diode; MMP, matrix metallopeptidase.

LED groups (P>0.05; Fig. 1B). Following MPPa-PDT treatment, the expression of the G_1/S phase checkpoint-associated proteins was partially downregulated, whereas the expression of G_2/M checkpoint-associated proteins was notably downregulated. These results were consistent with those obtained for MG-63 cells by flow cytometry, suggesting that MG-63 cell division was arrested at the G_2/M phase following MPPa-PDT treatment due to the inhibition of G_2/M cycle-related protein expression and thus cell proliferation.

MPPa-PDT inhibits the migration and invasion of MG-63 cells. To evaluate whether MPPa-PDT inhibited the migration and invasion of MG-63 cells, wound-healing and invasion assays using MG-63 cells were performed. The wound-healing

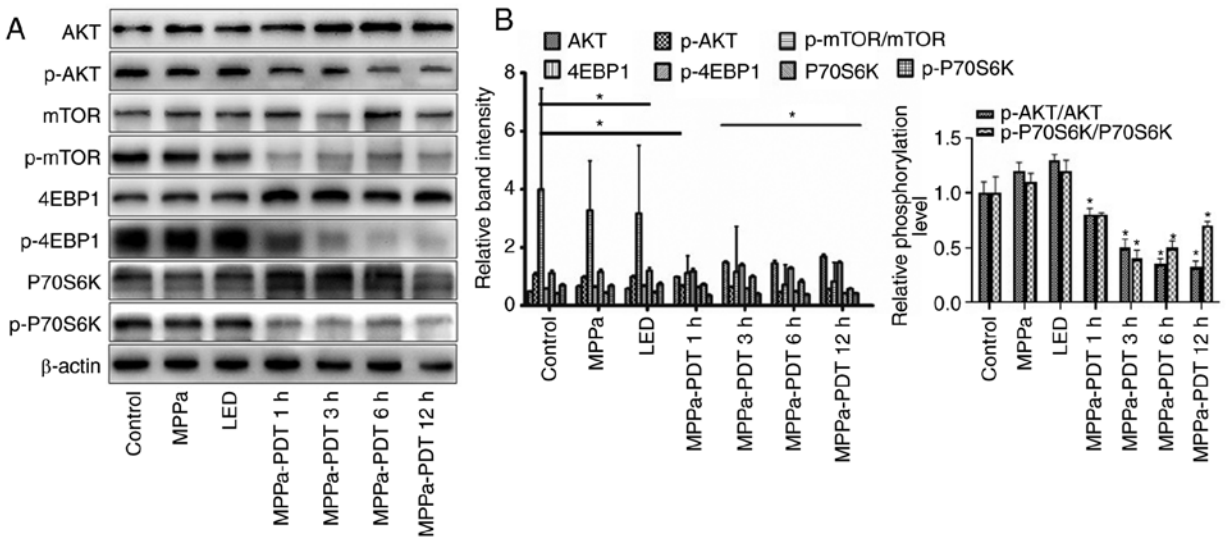

Figure 3. Effects of MPPa-PDT inhibition on the PI3K/Akt/mTOR signaling pathway. (A) p-Akt, Akt, p-mTOR, mTOR, p-4EBP1, 4EBP1, p-P70S6K and P70S6K protein expression levels were analyzed by western blotting analysis. (B) Densitometric analysis of protein expression. *P<0.05 vs. control. MPPa, pyropheophorbide-α methyl ester; PDT, photodynamic therapy; LED, cells treated with a light-emitting diode; p, phosphorylated; 4EBP1, eukaryotic translation initiation factor 4E-binding protein 1.

assay results demonstrated that following MPPa-PDT treatment, the cell migration distance was significantly shorter in the MPPa-PDT group compared with that in the control, MPPa and LED groups (P<0.05; Fig. 2A and C). No significant differences were observed in the migration distances among the control, MPPa and LED groups (P>0.05; Fig. 2A and C). Transwell invasion assay results demonstrated that after MPPa-PDT treatment, the number of transmembrane cells was significantly lower in the MPPa-PDT group compared with that in the control, MPPa and LED groups (P<0.05; Fig. 2B and D). No significant differences were observed in the numbers of cells among the control, MPPa and LED groups (P>0.05; Fig. 2B and D).

Further western blotting results demonstrated that following MPPa-PDT treatment, the expression levels of the migration-related protein E-cad in MG-63 cells were higher compared with those in the control, MPPa and LED groups. By contrast, expression of the invasion-related proteins MMP-2 and MMP-9 was decreased in the MPPa-PDT group compared with all other groups (P<0.05; Fig. 2E). No significant differences were observed among the control, MPPa and LED groups (P>0.05; Fig. 2E). The results were consistent with those from the MG-63 cell migration and invasion assays. These results suggested that MG-63 cell migration and invasion were inhibited by MPPa-PDT treatment.

Photodynamic inhibition of the AKT/mTOR pathway activation in MG-63 cells. Previous studies have demonstrated that the phosphoinositide 3-kinase (PI3K)/AKT/mTOR pathway serves an important role in tumor cell proliferation, angiogenesis and metastasis, as well as in the antagonism of radiotherapy and chemotherapy (24-26). To investigate whether MPPa-PDT inhibited the AKT/mTOR pathway activation, western blotting was performed. Following MPPa-PDT treatment, the levels of the p-AKT, p-mTOR, 4-EBP-1 and p-P70S6K proteins were significantly lower and the levels of the corresponding non-phosphorylated AKT, mTOR, 4-EBP-1 and P70S6K proteins were significantly higher in the MPPa-PDT group compared with the control, MPPa, and LED groups (P<0.05; Fig. 3A). However, no significant changes in protein expression were observed among the control, MPPa and LED groups (P>0.05; Fig. 4A). These results suggested that the phosphorylation and activation of the AKT/mTOR pathway proteins in MG-63 cells were inhibited by MPPa-PDT treatment.

MPPa-PDT induces MG-63 cell apoptosis. Following MPPa-PDT treatment, the apoptotic rate was significantly higher in the MPPa-PDT group compared with the control, MPPa and LED groups according to the flow cytometry assay (P<0.05; Fig. 4A), whereas no significant differences were observed among the control, MPPa and LED groups (P>0.05; Fig. 4A). Western blotting results indicated that cleaved caspase-3 and cleaved PARP expression increased after 3 h of MPPa-PDT treatment (P<0.05; Fig. 4B), but no notable changes were observed among the control, MPPa and LED groups (P>0.05; Fig. 4B). These results suggested that MPPa-PDT induced apoptosis in osteosarcoma MG-63 cells.

The ERS pathway is involved in MPPa-PDT-induced apoptosis in MG-63 cells. Flow cytometry assays were performed to investigate whether ERS contributed to the MPPa-PDT-induced apoptosis in osteosarcoma MG-63 cells. The intracellular calcium level was higher in the MPPa-PDT group compared with that in the control, MPPa and LED groups (P<0.05; Fig. 5A). No significant changes in the calcium ion levels were observed among the control, MPPa and LED groups (P>0.05; Fig. 5A). These results suggested that the MG-63 cells exhibited endoplasmic reticulum damage following MPPa-PDT treatment.

In addition, western blotting revealed that at 1, 3, 6 and 12 h after MPPa-PDT treatment, the expression levels of ERS-related proteins Bip, IRE1α, PERK, p-PERK and PDI and ERS-related apoptotic proteins CHOP and cleaved

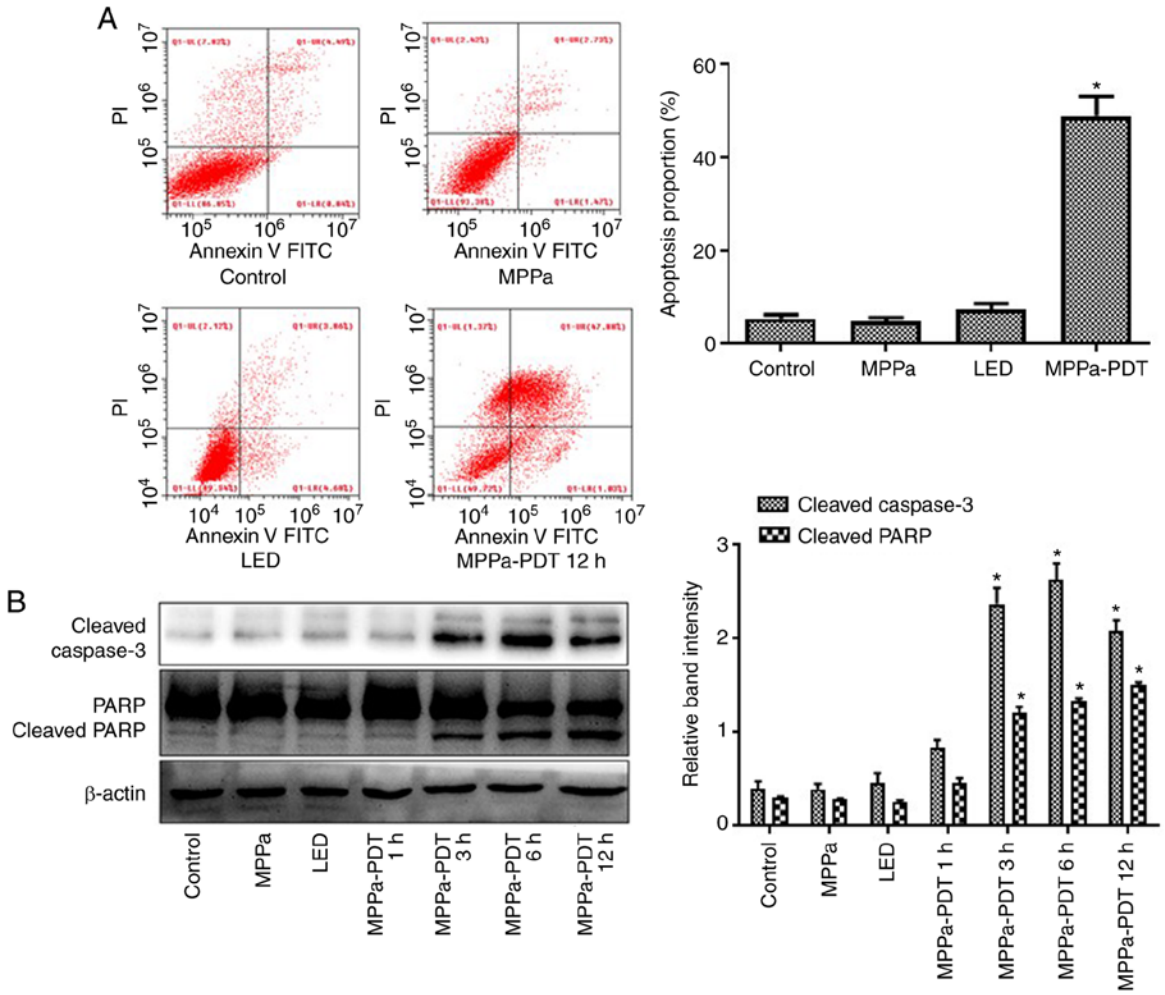

Figure 4. MPPa-PDT induces MG-63 cell apoptosis. (A) Following MPPa-PDT treatment for 12 h, apoptotic rates were analyzed by flow cytometry and calculated as the percentage of early apoptotic (Annexin V^+/PI^-) cells plus the percentage of late apoptotic (Annexin V^+/PI^+) cells. (B) At 12 h, whole-cell lysates were prepared to determine cleaved caspase-3 and cleaved PARP protein expression by western blotting. Data are presented as the mean ± SD from three independent experiments. *P<0.05 vs. control. MPPa, pyropheophorbide-α methyl ester; PDT, photodynamic therapy; LED, cells treated with a light-emitting diode; PI, propidium iodide; PARP, poly (ADP-ribose) polymerase 1.

caspase-12 were higher, whereas the expression level of PERK was lower in the MPPa-PDT-treated MG-63 cells compared with the control groups (P<0.05; Fig. 5B and C). No significant changes in these indicators were observed among the control, MPPa and LED groups (P>0.05; Fig. 5B and C). These results indicated that ERS was induced by MPPa-PDT in MG-63 cells and that ERS-induced apoptosis was involved in this process.

mTOR targeting promotes apoptosis by influencing photodynamic therapy-induced autophagy of osteosarcoma MG-63. mTOR is not only an important factor regulating cell growth and proliferation, but also a key promoter of autophagy that inhibits autophagy after activation (26,27). A previous study has demonstrated that MPPa-PDT can induce autophagy in MG-63 cells to promote apoptosis (13). The present study investigated whether the expression of autophagy-related proteins of MG-63 cells was altered following MPPa-PDT induction via mTOR phosphorylation inhibition to promote MG-63 cell apoptosis and reduce MPPa-PDT tolerance.

The flow cytometry assay results revealed that following pretreatment with RAPA, the numbers of apoptotic cells were significantly higher in the MPPA-PDT + RAPA group compared with the MPPa-PDT group (P<0.05; Fig. 6A), whereas no significant changes in apoptosis were observed in the RAPA and control groups (P>0.05; Fig. 6A). Western blotting results indicated that mTOR expression was downregulated and the p-mTOR phosphorylation level was further decreased in the MG-63 cells following RAPA pretreatment; the expression of the autophagy marker LC3-II was upregulated and P62 expression was downregulated in MG-63 cells treated with RAPA and MPPa-PDT compared with the control groups (P<0.05; Fig. 6B). The protein expression levels of cleaved caspase-3 and cleaved PARP were significantly increased (P<0.05; Fig. 6B), which was consistent with the apoptosis results of the flow cytometry assay. These results suggested that the addition of an mTOR phosphorylation inhibitor suppressed the autophagy of osteosarcoma MG-63 cells induced by photodynamic therapy and further promoted apoptosis and reduced the tolerance of MG-63 cells to MPPa-PDT.

Discussion

Currently, surgery combined with neoadjuvant chemotherapy is the main treatment for osteosarcoma, but the treatment

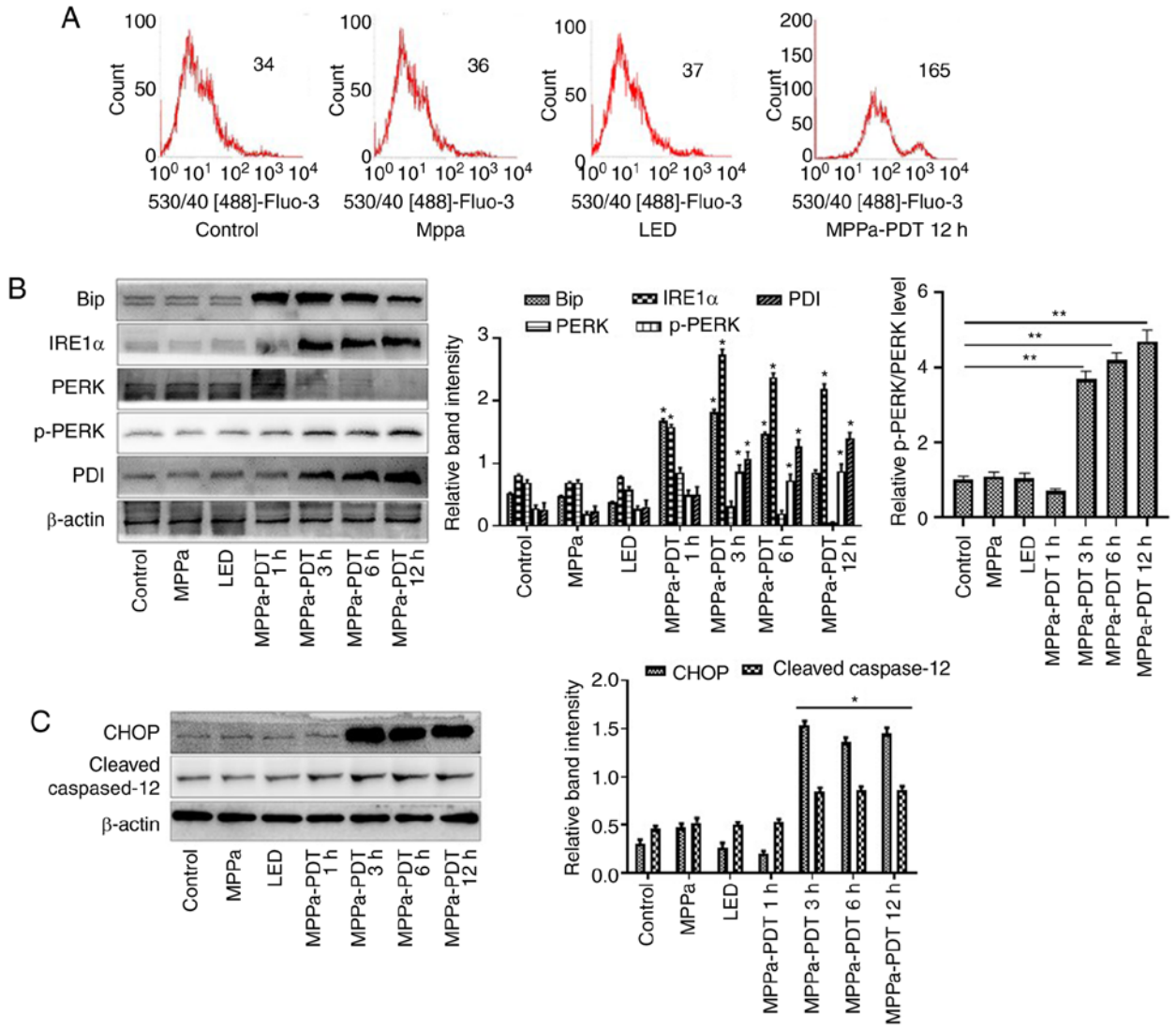

Figure 5. The ERS pathway is involved in MPPa-PDT-induced MG-63 cell apoptosis. (A) The calcium levels in the cells were measured by flow cytometry. (B and C) At 12 h, whole-cell lysates were prepared to determine the expression of (B) ERS-related proteins (Bip, IRE1α, PERK, p-PERK, and PDI) and (C) ERS-related apoptotic proteins (CHOP and cleaved caspase-12) by western blotting analysis. Data are presented as the mean ± SD from three independent experiments. *P<0.05 vs. control. MPPa, pyropheophorbide-α methyl ester; PDT, photodynamic therapy; LED, cells treated with a light-emitting diode; ERS, endoplasmic reticulum stress; IRE1α, serine/threonine-protein kinase/endoribonuclease IRE1; PERK, eukaryotic translation initiation factor 2α kinase 3; PDI, protein disulfide; CHOP, C/EBP-homologous protein 10.

remains problematic, including drug toxicity, side effects, a high recurrence rate, chemotherapy resistance and inoperability due to vascular nerve invasion (6). Therefore, new treatment methods are urgently needed in clinical practice. PDT is a promising new approach to cancer therapy that has been approved by the US Food and Drug Administration for the treatment of tumors (7). Previous studies have reported that PDT may inhibit the metastasis of osteosarcoma and restore the immune function of osteosarcoma cells (28,29). MPPa belongs to the second generation of photosensitizers and is a chlorophyll derivative (30). To date, MPPa-PDT has been used clinically for the treatment of a variety of tumors such as osteosarcoma, lung and cervical cancer (17,19,31). The present study aimed to explore the functional mechanism of MPPa-PDT in osteosarcoma.

The results of the present study suggested that MPPa-PDT inhibited cell cycle activity by arresting osteosarcoma MG-63 cells at the G_2/M phase. Previous studies have demonstrated that Cyclin D1 is an essential protein in the G_1 phase of cells; Cyclin E binds to CDK2 to form a complex that promotes cells into the S phase, whereas Cyclin A and Cyclin B1 are key proteins in the G_2/M phase (32-34). In the present study, compared with that in the control group, Cyclin D1 expression was not significantly different in the MPPa-PDT group, and the decrease in Cyclin E expression was consistent with the slight decrease in the proportion of cells in the G_1 phase observed in the flow cytometry analysis of the cell cycle. These results suggested that MPPa-PDT had a minimal effect on the G_1 phase of the cells. Cyclin A and Cyclin B1 protein expression was significantly downregulated, and the flow cytometry results demonstrated that the proportion of cells remaining in the G_2/M phase increased significantly following MPPa-PDT treatment compared with the other groups, which induced cell cycle arrest and inhibited cell proliferation.

Migration and invasion are the most prominent malignant features of osteosarcoma; human osteosarcoma MG-63 cells

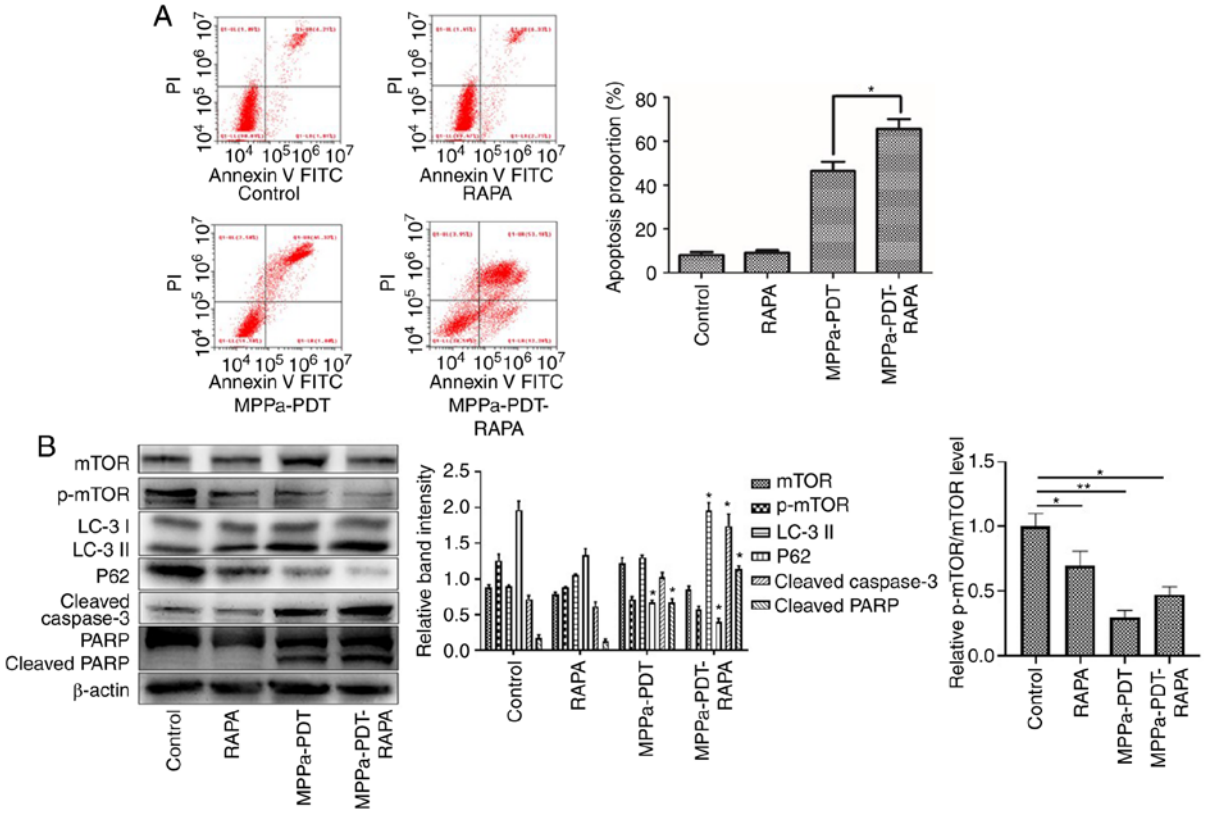

Figure 6. Apoptosis is promoted via mTOR to enhance MPPa-PDT-induced autophagy in MG-63 cells. MG-63 cells were pretreated with RAPA for 3 h in the presence or absence of MPPa-PDT. Control cells received no pretreatment or only RAPA pretreatment. (A) Following the corresponding treatment, apoptotic rates were measured by flow cytometry. The apoptotic rate was calculated as the percentage of early apoptotic (Annexin V^+/PI^-) cells plus the percentage of late apoptotic (Annexin V^+/PI^+) cells. (B) At 12 h after treatment, whole-cell lysates were prepared to determine p-mTOR, LC-3, P62, cleaved caspase-3 and cleaved PARP expression by western blotting. Data are presented as the mean ± SD from three independent experiments. $^*P<0.05$ and $^{**}P<0.01$. vs. MPPa-PDT. MPPa, pyropheophorbide-α methyl ester; PDT, photodynamic therapy; RAPA, rapamycin; PI, propidium iodide; PARP, poly (ADP-ribose) polymerase 1; LC-3, microtubule-associated protein 1 light chain 3α; p, phosphorylated.

exhibit strong migratory and invasive abilities (35,36). The results of the preset study demonstrated that the wound-healing ability of MG-63 cells and the number of transmembrane MG-63 cells were significantly decreased following MPPa-PDT treatment compared with the control groups, suggesting that MPPa-PDT significantly reduced the migratory and invasive abilities of osteosarcoma MG-63 cells *in vitro*. The E-cad protein serves an important role in the metastasis of malignant tumors, and the decrease in E-cad protein expression in tumor tissues leads to intercellular adhesion weakening, extracellular matrix degradation and basement membrane defects, which promote the release of tumor cells from their original positions and allow them to enter the blood and travel to distant sites (37,38). Zhang *et al* (39) reported that the specific inhibition of E-cad protein expression contributed to the distant metastasis of osteosarcoma MG-63 cells. The results of the present study demonstrated that E-cad protein expression was upregulated in osteosarcoma MG-63 cells following MPPa-PDT treatment. In addition, malignant tumors secrete MMPs and degrade the extracellular matrix (40). *In vivo*, MMPs interact with tissue inhibitors of metalloproteinases (TIMPs) to maintain the balance of extracellular matrix synthesis and degradation (41,42); however, MMP expression in malignant tumor cells is greater than TIMP expression, resulting in more extracellular matrix degradation than synthesis (43). Therefore, tumor cells are more susceptible to invasion and metastasis (40-43). Guo *et al* (44) demonstrated that tectorigenin significantly inhibited the invasion of osteosarcoma cells by downregulating MMP-2 and MMP-9 expression. MMP-2 and MMP-9 expression in osteosarcoma MG-63 cells was significantly decreased after MPPa-PDT treatment compared with the control cells in the present study. These results suggested that the migratory and invasive abilities of MG-63 cells were inhibited by MPPa-PDT treatment.

The PI3K/AKT/mTOR pathway is the main signaling pathway involved in protein synthesis. It is widely involved in cell proliferation, differentiation and migration, promotes cell cycle progression and regulates apoptosis and autophagy (45). Following PI3K activation, AKT phosphorylation activates downstream signaling molecules, such as mTOR, and exerts corresponding biological effects (24-26). Studies have demonstrated that mTOR is an important factor regulating cell growth and proliferation (24,27). Transient activation of the AKT/mTOR signaling pathway serves an important role in the development of a number of malignant tumors such as lung, colorectal and breast cancer; the downstream serine/threonine protein kinase P70S6K can increase the translation efficiency of 5'-mTOR mRNA after phosphorylation activation and promote protein biosynthesis, whereas 4EBP1 phosphorylation promotes its activation of the eIF4E protein following separation from eIF4E and thus initiates protein translation (46,47). The results of the present study demonstrated that phosphory-

lation of AKT, mTOR, 4EBP1 and P70S6K was reduced by MPPa-PDT treatment, which inhibited the AKT/mTOR pathway activity and decreased the quality and efficiency of protein biosynthesis in MG-63 cells. Indirectly, MPPa-PDT may inhibit the expression of cell cycle-associated proteins by blocking the AKT/mTOR pathway activity and thus the MG-63 cell cycle, thus inhibiting cell proliferation. Previous studies have reported that MPPa-PDT induced apoptosis in lung, cervical and breast cancer cells (17,18,30). In the present study, after MPPa-PDT treatment, flow cytometry assay results demonstrated that the apoptotic rate of the MPPa-PDT group was significantly increased. In addition, the expression of the apoptosis-related proteins cleaved caspase-3 and cleaved PARP was significantly enhanced. These results indicated that MPPa-PDT induced apoptosis in human osteosarcoma MG-63 cells.

The endoplasmic reticulum is a very complex organelle with the ability to control protein synthesis, transmembrane transport, integration, post-translational modifications, glycosylation modifications, phospholipid and cholesterol synthesis and intracellular calcium homeostasis. Under pathological conditions, the disturbance of endoplasmic reticulum function leads to ERS (48). ERS triggers an unfolded protein response and intracellular calcium homeostasis imbalance and increases the level of protein phosphorylation or expression by activating the endoplasmic reticulum transmembrane proteins PERK, IRE1α, and ATF6; this step activates downstream signaling molecules or gene expression and maintains cell homeostasis, which is essential for cell survival. However, persistent or excessive ERS promotes the expression of endoplasmic reticulum-associated death proteins and induces apoptosis (49-52). In the present study, the level of intracellular calcium in MG-63 cells was significantly increased after 3-h MPPa-PDT treatment. Western blotting results also indicated that Bip, IRE1α and p-PERK expression was significantly increased following MPPa-PDT treatment. The expression of the endoplasmic reticulum chaperone protein PDI was also upregulated to promote the proper folding of unfolded or misfolded proteins and to reduce cellular damage (48). The above results indicated that MPPa-PDT may induce ERS in human osteosarcoma MG-63 cells. CHOP, which is a member of the C/EBP transcription factor family, is an ERS-specific transcription factor, and increased expression of this protein mediates apoptosis (53). Caspase-12, which is a member of the caspase family, is located on the endoplasmic reticulum membrane and is a key molecule mediating stress-induced apoptosis in the endoplasmic reticulum; caspase-12 is activated and cleaved only when ERS-related apoptosis occurs and mediates further apoptosis (51). In the present study, CHOP and cleaved caspase-12 expression in MG-63 cells was significantly increased after MPPa-PDT treatment compared with the control groups. These results indicated that MPPa-PDT induced ERS in MG-63 cells and upregulated CHOP and cleaved caspase-12 expression, which activated the ERS apoptosis pathway and ultimately induced apoptosis.

The sensitivity of MG-63 cells to MPPa-PDT was enhanced using mTOR as an intervention target to influence autophagy, promote osteosarcoma cell apoptosis and increase the effect of MPPa-PDT. The mTOR molecule is a key promoter of the autophagy process and can downregulate cellular autophagy activity upon activation (54,55). A previous study reported that autophagy induced by MPPa-PDT promoted MG-63 cell apoptosis (13). Following the addition of RAPA, which is a phosphorylation inhibitor of mTOR, the degree of mTOR phosphorylation was further inhibited, the expression of autophagy-related proteins was significantly altered, and the apoptotic rate of the MG-63 cells was further enhanced compared with MPPa-PDT treatment alone. Therefore, with mTOR as a target, the effects of MPPa-PDT on MG-63 cells can be improved by downregulating the degree of mTOR phosphorylation.

In conclusion, the results of the present study demonstrated that MPPa-PDT blocked the MG-63 cell cycle, inhibited cell migration, invasion and the AKT/mTOR pathway activation, and induced ERS and ERS-induced apoptosis in MG-63 cells. At the same time, mTOR may enhance the effects of MPPa-PDT on MG-63 cells as an intervention target. These results enrich our understanding of MPPa-PDT in the treatment of osteosarcoma cells; however, the present results and targets of MPPa-PDT for the treatment of osteosarcoma require further studies in multiple cell lines and *in vivo* experiments prior to clinical application.

Acknowledgements

The human fibroblast HFL-1 cell line was donated by Professor Zhou Jing, Department of Respiratory, the First Affiliated Hospital of Chongqing Medical University (Chongqing, China).

Funding

This study was supported by the National Natural Science Foundation of China (81572634).

Availability of data and materials

The datasets used and/or analyzed during the current study are available from the corresponding author on reasonable request.

Authors' contributions

YC and HY performed the experimental work, data collection and interpretation. YT and YO participated in the design and coordination of the experimental work and the acquisition of data. SZ and HYY participated in the study design, data collection and analysis and manuscript preparation. JL and ZB participated in the study design, analyzed and interpreted the data and drafted the manuscript. All authors read and approved the manuscript and agree to be accountable for all aspects of the research in ensuring that the accuracy and integrity of any part of the work are appropriately investigated and resolved.

Ethics approval and consent to participate

Not applicable.

Patient consent for publication

Not applicable.

Competing interests

The authors declare that they have no competing interests.

References

1. Ando K, Heymann MF, Stresing V, Mori K, Redini F and Heymann D: Current therapeutic strategies and novel approaches in osteosarcoma. Cancers (Basel) 5: 591-616, 2013.
2. Yu W, Wang Y, Zhu J, Jin L, Liu B, Xia K, Wang J, Gao J, Liang C and Tao H: Autophagy inhibitor enhance ZnPc/BSA nanoparticle induced photodynamic therapy by suppressing PD-L1 expression in osteosarcoma immunotherapy. Biomaterials 192: 128-39, 2019.
3. Arai K, Sakamoto R, Kubota D and Kondo T: Proteomic approach toward molecular backgrounds of drug resistance of osteosarcoma cells in spheroid culture system. Proteomics 13: 2351-2360, 2013.
4. Cao D, Zhu W, Kuang Y and Zhao S: A safe and effective treatment: Surgery combined with photodynamic therapy for multiple basal cell carcinomas. Photodiagnosis Photodyn Ther 28: 133-135, 2019.
5. Wang X, Ramamurthy G, Shirke AA, Walker E, Mangadlao J, Wang Z, Wang Y, Shan L, Schluchter MD, Dong Z, *et al*: Photodynamic therapy is an effective adjuvant therapy for image-guided surgery in prostate cancer. Cancer Res 80: 156-162, 2020.
6. Wu ZJ, Tan JC, Qin X, Liu B and Yuan ZC: Significance of circulating tumor cells in osteosarcoma patients treated by neoadjuvant chemotherapy and surgery. Cancer Manag Res 10: 3333-3339, 2018.
7. Nishie H, Kataoka H, Yano S, Yamaguchi H, Nomoto A, Tanaka M, Kato A, Shimura T, Mizoshita T, Kubota E, *et al*: Excellent antitumor effects for gastrointestinal cancers using photodynamic therapy with a novel glucose conjugated chlorin e6. Biochem Biophys Res Commun 496: 1204-1209, 2018.
8. Savoia P, Deboli T, Previgliano A and Broganelli P: Usefulness of photodynamic therapy as a possible therapeutic alternative in the treatment of basal cell carcinoma. Int J Mol Sci 16: 23300-23317, 2015.
9. Phuong PTT, Lee S, Lee C, Seo B, Park S, Oh KT, Lee ES, Choi HG, Shin BS and Youn YS: Beta-carotene-bound albumin nanoparticles modified with chlorin e6 for breast tumor ablation based on photodynamic therapy. Colloids Surf B Biointerfaces 171: 123-133, 2018.
10. Fujishiro T, Nonoguchi N, Pavliukov M, Ohmura N, Kawabata S, Park Y, Kajimoto Y, Ishikawa T, Nakano I and Kuroiwa T: 5-Aminolevulinic acid-mediated photodynamic therapy can target human glioma stem-like cells refractory to antineoplastic agents. Photodiagnosis Photodyn Ther 24: 55-68, 2018.
11. Kessel D and Oleinick NL: Cell death pathways associated with photodynamic therapy: An update. Photochem Photobiol 94: 213-218, 2018.
12. Zhang Q and Li L: Photodynamic combinational therapy in cancer treatment. J BUON 23: 561-567, 2018.
13. Huang Q, Ou YS, Tao Y, Yin H and Tu PH: Apoptosis and autophagy induced by pyropheophorbide-α methyl ester-mediated photodynamic therapy in human osteosarcoma MG-63 cells. Apoptosis 21: 749-760, 2016.
14. Chang JE, Yoon IS, Sun PL, Yi E, Jheon S and Shim CK: Anticancer efficacy of photodynamic therapy with hematoporphyrin-modified, doxorubicin-loaded nanoparticles in liver cancer. J Photochem Photobiol B 140: 49-56, 2014.
15. Silva AP, Kurachi C, Bagnato VS and Inada NM: Fast elimination of onychomycosis by hematoporphyrin derivative-photodynamic therapy. Photodiagnosis Photodyn Ther 10: 328-330, 2013.
16. Zeng H, Sun M, Zhou C, Yin F, Wang Z, Hua Y and Cai Z: Hematoporphyrin monomethyl ether-mediated photodynamic therapy selectively kills sarcomas by inducing apoptosis. PLoS One 8: e77727, 2013.
17. Tao Y, Ou Y, Yin H, Chen Y, Zhong S, Gao Y, Zhao Z, He B, Huang Q and Deng Q: Establishment and characterization of human osteosarcoma cells resistant to pyropheophorbide-α methyl ester-mediated photodynamic therapy. Int J Oncol 51: 1427-1438, 2017.
18. Qian G, Wang L, Zheng X and Yu T: Deactivation of cisplatin-resistant human lung/ovary cancer cells with pyropheophorbide-α methyl ester-photodynamic therapy. Cancer Biol Ther 18: 984-989, 2017.
19. Tu PH, Huang WJ, Wu ZL, Peng QZ, Xie ZB, Bao J and Zhong MH: Induction of cell death by pyropheophorbide-α methyl ester-mediated photodynamic therapy in lung cancer A549 cells. Cancer Med 6: 631-639, 2017.
20. Zhu J, Tian S, Li KT, Chen Q, Jiang Y, Lin HD, Yu LH and Bai DQ: Inhibition of breast cancer cell growth by methyl pyropheophenylchlorin photodynamic therapy is mediated though endoplasmic reticulum stress-induced autophagy in vitro and vivo. Cancer Med 7: 1908-1920, 2018.
21. Tu PH, Huang WJ, Wu ZL, Peng QZ, Xie ZB, Bao J and Zhong MH: Induction of cell death by pyropheophorbide-α methyl ester-mediated photodynamic therapy in lung cancer A549 cells. Cancer Med 6: 631-639, 2017.
22. Tian Y, Leung W, Yue K and Mak N: Cell death induced by MPPa-PDT in prostate carcinoma in vitro and in vivo. Biochem Biophys Res Commun 348: 413-420, 2006.
23. de Miguel GC, Abrantes AM, Laranjo M, Grizotto AYK, Camporeze B, Pereira JA, Brites G, Serra A, Pineiro M, Rocha-Gonsalves A, *et al*: A new therapeutic proposal for inoperable osteosarcoma: Photodynamic therapy. Photodiagnosis Photodyn Ther 21: 79-85, 2018.
24. Gao W, Wu XL, Li DZ and Liu HD: HOTTIP participates in mammary cancer by promoting cell proliferation via PI3K/AKT pathway. Eur Rev Med Pharmacol Sci 22: 4181-4187, 2018.
25. Liu HW, Bi WT, Huang HT, Li RX, Xi Q, Feng L, Bo W, Hu M and Wen WS: Satb1 promotes Schwann cell viability and migration via activation of PI3K/AKT pathway. Eur Rev Med Pharmacol Sci 22: 4268-4277, 2018.
26. Wang J, Sun P, Chen Y, Yao H and Wang S: Novel 2-phenyloxypyrimidine derivative induces apoptosis and autophagy via inhibiting PI3K pathway and activating MAPK/ERK signaling in hepatocellular carcinoma cells. Sci Rep 8: 10923, 2018.
27. Lijun J, Shan H, Xiaoran Y, Zan Y, Guo Y and Han L: Quercetin suppresses the mobility of breast cancer by suppressing glycolysis through Akt-mTOR pathway mediated autophagy induction. Life Sci 208: 123-130, 2018.
28. Meier D, Botter SM, Campanile C, Robl B, Gräfe S, Pellegrini G, Born W and Fuchs B: Foscan and foslip based photodynamic therapy in osteosarcoma, in vitro, and in intratibial mouse models. Int J Cancer 140: 1680-1692, 2017.
29. Zhang F, Zhu Y, Fan G and Hu S: Photodynamic therapy reduces the inhibitory effect of osteosarcoma cells on dendritic cells by upregulating HSP70. Oncol Lett 16: 5034-5040, 2018.
30. Huang L, Lin H, Chen Q, Yu L and Bai D: MPPa-PDT suppresses breast tumor migration/invasion by inhibiting Akt-NF-κB-dependent MMP-9 expression via ROS. BMC Cancer 19: 1159, 2019.
31. Li W, Tan G, Cheng J, Zhao L, Wang Z and Jin Y: A novel photosensitizer 3^1,13^1-phenylhydrazine-Mppa (BPHM) and Its in vitro photodynamic therapy against HeLa cells. Molecules 21: pii: E558, 2016.
32. Santti K, Ihalainen H, Rönty M, Böhling T, Karlsson C and Haglund C: High cyclin A expression, but not Ki67, is associated with early recurrence in desmoid tumors. J Surg Oncol 118: 192-198, 2018.
33. Lal N, Nemaysh V and Luthra PM: Proteasome mediated degradation of CDC25C and Cyclin B1 in Demethoxycurcumin treated human glioma U87 MG cells to trigger G2/M cell cycle arrest. Toxicol Appl Pharmacol 356: 76-89, 2018.
34. Marampon F, Gravina G, Ju X, Vetuschi A, Sferra R, Casimiro M, Pompili S, Festuccia C, Colapietro A, Gaudio E, *et al*: Cyclin D1 silencing suppresses tumorigenicity, impairs DNA double strand break repair and thus radiosensitizes androgen-independent prostate cancer cells to DNA damage. Oncotarget 7: 5383-5400, 2016.
35. Cai H, Miao M and Wang Z: miR-214-3p promotes the proliferation, migration and invasion of osteosarcoma cells by targeting CADM1. Oncol Lett 16: 2620-2628, 2018.
36. Qiu J, Zhang Y, Chen H and Guo Z: MicroRNA-488 inhibits proliferation, invasion and EMT in osteosarcoma cell lines by targeting aquaporin 3. Int J Oncol 53: 1493-1504, 2018.
37. Campbell K and Casanova J: A role for E-cadherin in ensuring cohesive migration of a heterogeneous population of non-epithelial cells. Nat Commun 6: 7998, 2015.
38. Shan Z, Wei Z and Shaikh ZA: Suppression of ferroportin expression by cadmium stimulates proliferation, EMT, and migration in triple-negative breast cancer cells. Toxicol Appl Pharmacol 356: 36-43, 2018.
39. Zhang LZ, Mei J, Qian ZK, Cai XS, Jiang Y and Huang WD: The role of VE-cadherin in osteosarcoma cells. Pathol Oncol Res 16: 111-117, 2010.

40. Li F, Zhang J, Guo J, Jia Y, Han Y and Wang Z: RNA interference targeting CD147 inhibits metastasis and invasion of human breast cancer MCF-7 cells by downregulating MMP-9/VEGF expression. Acta Biochim Biophys Sin (Shanghai) 50: 676-684, 2018.
41. Liao CL, Chu YL, Lin HY, Chen CY, Hsu MJ, Liu KC, Lai KC, Huang AC and Chung JG: Bisdemethoxycurcumin suppresses migration and invasion of human cervical cancer HeLa cells via inhibition of NF-κB, MMP-2 and -9 pathways. Anticancer Res 38: 3989-3997, 2018.
42. Xu M, Jiang H, Wang H, Liu J, Liu B and Guo Z: SB225002 inhibits prostate cancer invasion and attenuates the expression of BSP, OPN and MMP-2. Oncol Rep 40: 726-736, 2018.
43. Shimoda M, Jackson HW and Khokha R: Tumor suppression by stromal TIMPs. Mol Cell Oncol 3: e975082, 2016.
44. Guo Y, Chen YH, Cheng ZH, Ou-Yang HN, Luo C and Guo ZL: Tectorigenin inhibits osteosarcoma cell migration through downregulation of matrix metalloproteinases in vitro. Anticancer Drugs 27: 540-546, 2016.
45. Liu JZ, Hu YL, Feng Y, Guo YB, Liu YF, Yang JL, Mao QS and Xue WJ: Rafoxanide promotes apoptosis and autophagy of gastric cancer cells by suppressing PI3K/Akt/mTOR pathway. Exp Cell Res 385: 111691, 2019.
46. Zhou M, Shen S, Zhao X and Gong X: Luteoloside induces G0/G1 arrest and pro-death autophagy through the ROS-mediated AKT/mTOR/p70S6K signalling pathway in human non-small cell lung cancer cell lines. Biochem Biophys Res Commun 494: 263-269, 2017.
47. Zhu Y, Rao Q, Zhang X and Zhou X: Galangin induced antitumor effects in human kidney tumor cells mediated via mitochondrial mediated apoptosis, inhibition of cell migration and invasion and targeting PI3K/AKT/mTOR signalling pathway. J BUON 23: 795-799, 2018.
48. Santamaria PG, Mazón MJ, Eraso P and Portillo F: UPR: An upstream signal to EMT induction in cancer. J Clin Med 8: pii: E624, 2019.
49. Santofimia-Castaño P, Izquierdo-Alvarez A, Plaza-Davila M, Martinez-Ruiz A, Fernandez-Bermejo M, Mateos-Rodriguez JM, Salido GM and Gonzalez A: Ebselen impairs cellular oxidative state and induces endoplasmic reticulum stress and activation of crucial mitogen-activated protein kinases in pancreatic tumour AR42J cells. J Cell Biochem 119: 1122-1133, 2018.
50. Hetz C and Saxena S: ER stress and the unfolded protein response in neurodegeneration. Nat Rev Neurol 13: 477-491, 2017.
51. Badiola N, Penas C, Miñano-Molina A, Barneda-Zahonero B, Fadó R, Sánchez-Opazo G, Comella JX, Sabriá J, Zhu C, Blomgren K, *et al*: Induction of ER stress in response to oxygen-glucose deprivation of cortical cultures involves the activation of the PERK and IRE-1 pathways and of caspase-12. Cell Death Dis 2: e149, 2011.
52. Guha P, Kaptan E, Gade P, Kalvakolanu DV and Ahmed H: Tunicamycin induced endoplasmic reticulum stress promotes apoptosis of prostate cancer cells by activating mTORC1. Oncotarget 8: 68191-68207, 2017.
53. Sidhu A, Miller JR, Tripathi A, Garshott DM, Brownell AL, Chiego DJ, Arevang C, Zeng Q, Jackson LC, Bechler SA, *et al*: Borrelidin induces the unfolded protein response in oral cancer cells and chop-dependent apoptosis. ACS Med Chem Lett 6: 1122-1127, 2015.
54. Zhou J, Tan SH, Nicolas V, Bauvy C, Yang ND, Zhang J, Xue Y, Codogno P and Shen HM: Activation of lysosomal function in the course of autophagy via mTORC1 suppression and autophagosome-lysosome fusion. Cell Res 23: 508-523, 2013.
55. Tao YF, Li ZH, Du WW, Xu LX, Ren JL, Li XL, Fang F, Xie Y, Li M, Qian GH, *et al*: Inhibiting PLK1 induces autophagy of acute myeloid leukemia cells via mammalian target of rapamycin pathway dephosphorylation. Oncol Rep 37: 1419-1429, 2017.

This work is licensed under a Creative Commons Attribution-NonCommercial-NoDerivatives 4.0 International (CC BY-NC-ND 4.0) License.